Available online at www.sciencedirect.com
ScienceDirect
Journal of Solid State Chemistry 180 (2007) 1068–1075
JOURNAL OF SOLID STATE CHEMISTRY
www.elsevier.com/locate/jssc

Structural properties of a family of hydrogen-bonded co-crystals formed between gemfibrozil and hydroxy derivatives of *t*-butylamine, determined directly from powder X-ray diffraction data

Eugene Y. Cheung[a], Sarah E. David[b], Kenneth D.M. Harris[a,*], Barbara R. Conway[b], Peter Timmins[c]

[a]*School of Chemistry, Cardiff University, Park Place, Cardiff CF10 3AT, Wales, UK*
[b]*School of Life and Health Sciences, Aston University, Aston Triangle, Birmingham B4 7ET, UK*
[c]*Bristol-Myers Squibb, Pharmaceutical Research Institute, Wirral, Merseyside CH46 1QW, UK*

Received 8 October 2006; received in revised form 27 December 2006; accepted 30 December 2006
Available online 14 January 2007

Abstract

We report the formation and structural properties of co-crystals containing gemfibrozil and hydroxy derivatives of *t*-butylamine $H_2NC(CH_3)_{3-n}(CH_2OH)_n$, with $n = 0$, 1, 2 and 3. In each case, a 1:1 co-crystal is formed, with transfer of a proton from the carboxylic acid group of gemfibrozil to the amino group of the *t*-butylamine derivative. All of the co-crystal materials prepared are polycrystalline powders, and do not contain single crystals of suitable size and/or quality for single crystal X-ray diffraction studies. Structure determination of these materials has been carried out directly from powder X-ray diffraction data, using the direct-space Genetic Algorithm technique for structure solution followed by Rietveld refinement. The structural chemistry of this series of co-crystal materials reveals well-defined structural trends within the first three members of the family ($n = 0$, 1, 2), but significantly contrasting structural properties for the member with $n = 3$.

Keywords: Structure determination; Powder X-ray diffraction; Genetic algorithm; Co-crystal; Hydrogen bonding

1. Introduction

Gemfibrozil [2,2-dimethyl-5-(2,5-xylyloxy)valeric acid; denoted **1**; Fig. 1] has received considerable attention within pharmaceutical sciences, particularly with regard to its properties as a cholesterol-lowering drug [1]. We explore here the formation of co-crystals containing gemfibrozil and members of a family of hydroxy derivatives of *t*-butylamine $H_2NC(CH_3)_{3-n}(CH_2OH)_n$, with $n = 0$, 1, 2 and 3 (denoted **A**–**D** respectively; Fig. 1) under the expectation that these materials will exhibit interesting structural chemistry. In particular, systematic variation of the number of hydroxyl groups within the *t*-butylamine derivative provides the opportunity to explore structural trends in the hydrogen bonding arrangements within the family of co-crystal materials.

As reported below, co-crystal materials are found to be formed between **1** and each of the molecules **A**–**D** in a 1:1 stoichiometric ratio. These co-crystals are denoted **1A**–**1D** respectively. In each case, the co-crystal contains deprotonated **1** as the anion and protonated **A**–**D** as the cation, resulting from transfer of a proton from the carboxylic acid group of **1** to the amino group of **A**–**D**. All of the co-crystal materials **1A**–**1D** obtained were polycrystalline powders, and did not contain single crystals of suitable size and/or quality for single crystal X-ray diffraction studies. In such cases, structure determination must instead be carried out using powder X-ray diffraction data. Fortunately, new opportunities have arisen within the last decade or so for carrying out complete structure determination of organic molecular solids directly from powder X-ray diffraction data [2], particularly by employing the direct-space strategy

*Corresponding author. Fax: +44 29 2087 4030.
E-mail address: HarrisKDM@cardiff.ac.uk (K.D.M. Harris).

0022-4596/$ - see front matter © 2007 Elsevier Inc. All rights reserved.
doi:10.1016/j.jssc.2006.12.036

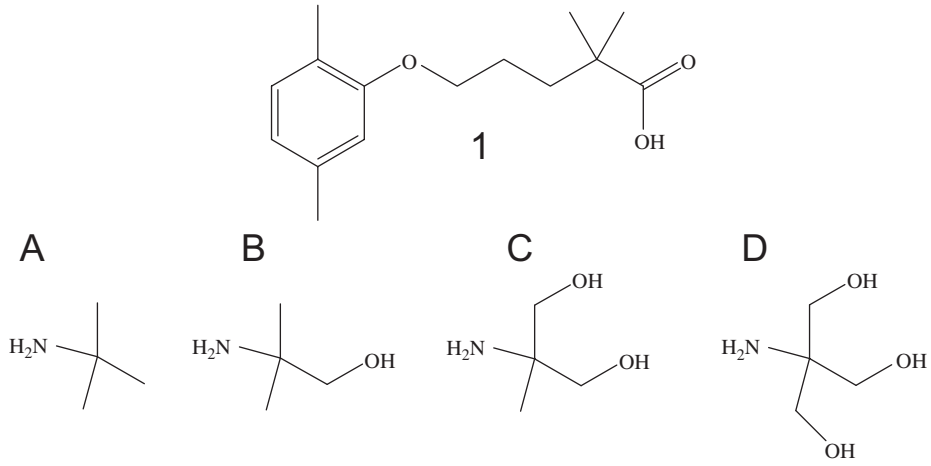

Fig. 1. Molecular structures of gemfibrozil (**1**) and molecules of the type $H_3NC(CH_3)_{3-n}(CH_2OH)_n$ with $n = 0, 1, 2, 3$ (**A**–**D** respectively).

for structure solution [3]. In the present work, this approach has been employed to determine the crystal structure of each of the co-crystal materials **1A**–**1D** from powder X-ray diffraction data, using the direct-space Genetic Algorithm technique for structure solution [4] followed by Rietveld refinement [5]. While the present work has been motivated by the interesting structural chemistry exhibited by systematic variation of the hydrogen-bonding opportunities within the series of co-crystals **1A**–**1D**, we note that, in general terms, there is increasing interest in the formation of co-crystalline phases of drug substances [6] (including co-crystal salts of the type discussed in this paper) as a potential route towards optimization of properties of relevance to their pharmaceutical applications.

2. Structure determination of organic solids from powder X-ray diffraction data

Crystal structure determination from powder X-ray diffraction data involves four stages: (i) unit cell determination, (ii) pattern-decomposition/profile-fitting (commonly carried out using the techniques of Pawley [7] or Le Bail [8]), (iii) structure solution, and (iv) structure refinement. The aim of structure solution is to derive a good approximation to the structure, using knowledge of the unit cell and space group determined in stages (i) and (ii), but starting with no knowledge of the actual arrangement of atoms or molecules within the unit cell. If the structure solution is sufficiently close to the true structure, a good quality structure can then be obtained by structure refinement, which is generally carried out using the Rietveld profile refinement technique.

Among recent developments in techniques for carrying out structure solution from powder X-ray diffraction data, the direct-space strategy is particularly suitable in the case of organic molecular materials. In the direct-space strategy, trial crystal structures are generated in direct space, and the quality of each trial structure is assessed by direct comparison between the powder X-ray diffraction pattern calculated for the trial structure and the experimental powder X-ray diffraction pattern. In our work, this comparison is carried out using the weighted powder profile *R*-factor R_{wp}, which takes peak overlap implicitly into consideration. In the present paper, our Genetic Algorithm (GA) technique [4], implemented in the program EAGER [9], was used to search for the structure representing the global minimum in R_{wp} in the direct-space structure solution calculation.

In the GA technique, a population of trial structures is allowed to evolve subject to the types of evolutionary operations (mating, mutation and natural selection) that govern evolution in biological systems. Each structure in the population is specified by its "genetic code", which represents, for each molecule in the asymmetric unit, the position $\{x, y, z\}$ and orientation $\{\theta, \varphi, \psi\}$ of the molecule in the unit cell, and the molecular conformation, defined by n variable torsion angles $\{\tau_1, \tau_2, \ldots, \tau_n\}$ (we note that hydrogen atoms are generally not included in structure solution calculations using powder X-ray diffraction data). Thus, in general, each molecular fragment is represented by $6+n$ structural variables, where n is the number of variable torsion angles required to define the molecular conformation. The quality ("fitness") of each structure in the population is assessed from its value of R_{wp} (in practice, fitness is defined as an appropriate decreasing function of R_{wp}). New structures are generated by the mating and mutation operations. In the natural selection procedure, only the structures of highest fitness (i.e. lowest R_{wp}) are allowed to pass from one generation to the next generation. After the population has evolved for a sufficient number of generations, the best structure in the population (i.e. the structure with lowest R_{wp}) should be close to the correct crystal structure, and is used as the starting structural model for Rietveld refinement. In the present work, Rietveld refinement was carried out using the GSAS program package [10].

3. Experimental

Gemfibrozil was supplied by DiPharma (Italy) and was of USP-BP grade. The *t*-butylamine derivatives **A**–**D** were obtained from Sigma-Aldrich. To prepare the co-crystals **1A** and **1B**, separate solutions were prepared containing **1** (0.01 moles) in acetonitrile (40 ml) and **A** or **B** (0.01 moles) in acetonitrile (40 ml). The solutions were then mixed, leading to the formation of a polycrystalline material, which was recovered by filtration under vacuum (if crystallization did not occur immediately, the solution was stored at −4 °C for ca. 12 h, which then led to the formation of a polycrystalline material). The recovered materials were dried at 40 °C for ca. 12 h under vacuum. To prepare the co-crystals **1C** and **1D**, a warm solution of **C** or **D** (0.01 moles) in methanol (40 ml) was prepared, and then mixed with a solution of **1** (0.01 moles) in acetonitrile (40 ml); the polycrystalline material that formed was collected and dried as described above. The samples of all co-crystal materials were stored in sealed containers at ambient temperature.

Powder X-ray diffraction data were recorded at ambient temperature in transmission mode on a Bruker D8 diffractometer for **1A** and **1B** (capillary sample holder; Ge-monochromated Cu$K\alpha_1$ radiation; VANTEC detector covering 12° in 2θ; 2θ range 5–70° for **1A** and 5–65° for **1B**; step size 0.01672°; total data collection time 12 h) and on a Siemens D5000 diffractometer for **1C** and **1D** (foil sample holder; Ge-monochromated Cu$K\alpha_1$ radiation; Braun PSD detector covering 8° in 2θ; 2θ range 5–70°; step size 0.02029°; total data collection time 10.5 h). Details of the structure determination calculations using these powder X-ray diffraction data are discussed below.

Fourier-transform infrared (FTIR) spectra were recorded for samples of **1A**–**1D** dispersed in KBr disks, using a Unicam Mattson 3000 FTIR spectrometer. The IR spectra exhibit characteristic vibration frequencies for $-CO_2^-$ and $-NH_3^+$ groups, confirming that the co-crystals **1A**–**1D** are salts comprising deprotonated **1** as the anion and protonated **A**–**D** as the cation [11].

4. Structure determination

The powder X-ray diffraction pattern of **1A** was indexed using the program KOHL [12], giving the following unit cell ($M_{20} = 26.4$, $F_{20} = 65.1$) with orthorhombic metric symmetry: $a = 6.44$ Å, $b = 9.67$ Å, $c = 33.10$ Å ($V = 2064$ Å^3). From systematic absences, the space group was assigned as $P2_12_12_1$. Le Bail fitting of the powder X-ray diffraction pattern using this unit cell and space group gave acceptable agreement between calculated and experimental data ($R_{wp} = 0.0237$, $R_p = 0.0141$). Structure solution was carried out using a single-population GA implemented in the program EAGER [9], with two structural fragments in the asymmetric unit representing the molecules **1** and **A**. The structural fragment representing **1** was defined by 12 structural variables, including six variable torsion angles (Fig. 2). The structural fragment representing **A** was defined by six structural variables, with no variable torsion angles. Thus, the total number of structural variables in the GA calculation was 18. The best trial structure ($R_{wp} = 0.0397$) obtained after 70 generations was used as the initial structural model for Rietveld refinement. In the Rietveld refinement, standard restraints on bond lengths and bond angles were used, and hydrogen atoms were placed in calculated positions towards the final stages of the refinement. The final refinement (Fig. 3a) gave $R_{wp} = 0.0258$, $R_p = 0.0177$, $R_{F^2} = 0.252$ and $\chi^2 = 3.97$ [$P2_12_12_1$; $a = 6.44807(31)$ Å, $b = 9.6811(4)$ Å, $c = 33.0974(14)$ Å].

The powder X-ray diffraction pattern of **1B** was indexed using the program ITO [13], giving the following unit cell ($M_{20} = 10.7$, $F_{20} = 87.0$) with monoclinic metric symmetry: $a = 26.87$ Å, $b = 6.37$ Å, $c = 23.90$ Å, $\beta = 91.7°$ ($V = 4090$ Å^3). From systematic absences, the space group was assigned as $C2/c$. Le Bail fitting using this unit cell gave an acceptable fit to the experimental powder X-ray diffraction pattern ($R_{wp} = 0.0197$, $R_p = 0.0134$). Structure solution was carried out using a parallel GA implemented in the program EAGER, with two structural fragments in the asymmetric unit representing the molecules **1** and **B**. The structural fragment representing **1** was defined by 12 variables, including six variable torsion angles, and the structural fragment representing **B** was defined by seven variables, including one variable torsion angle (Fig. 2). Thus, the total number of structural variables in the GA calculation was 19. The best trial structure ($R_{wp} = 0.0488$) after 41 generations was used as the initial structural model for Rietveld refinement, which was carried out as described above for **1A**. The final refinement (Fig. 3b)

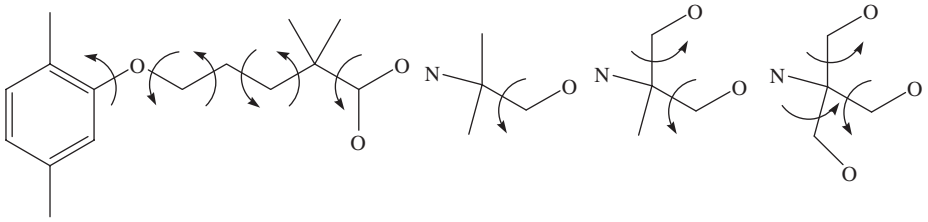

Fig. 2. Molecular fragments of (from left to right) **1**, **B**, **C** and **D** used in the direct-space structure solution calculations, with the variable torsion angles indicated by arrows. Note that hydrogen atoms are not included in the structure solution calculations.

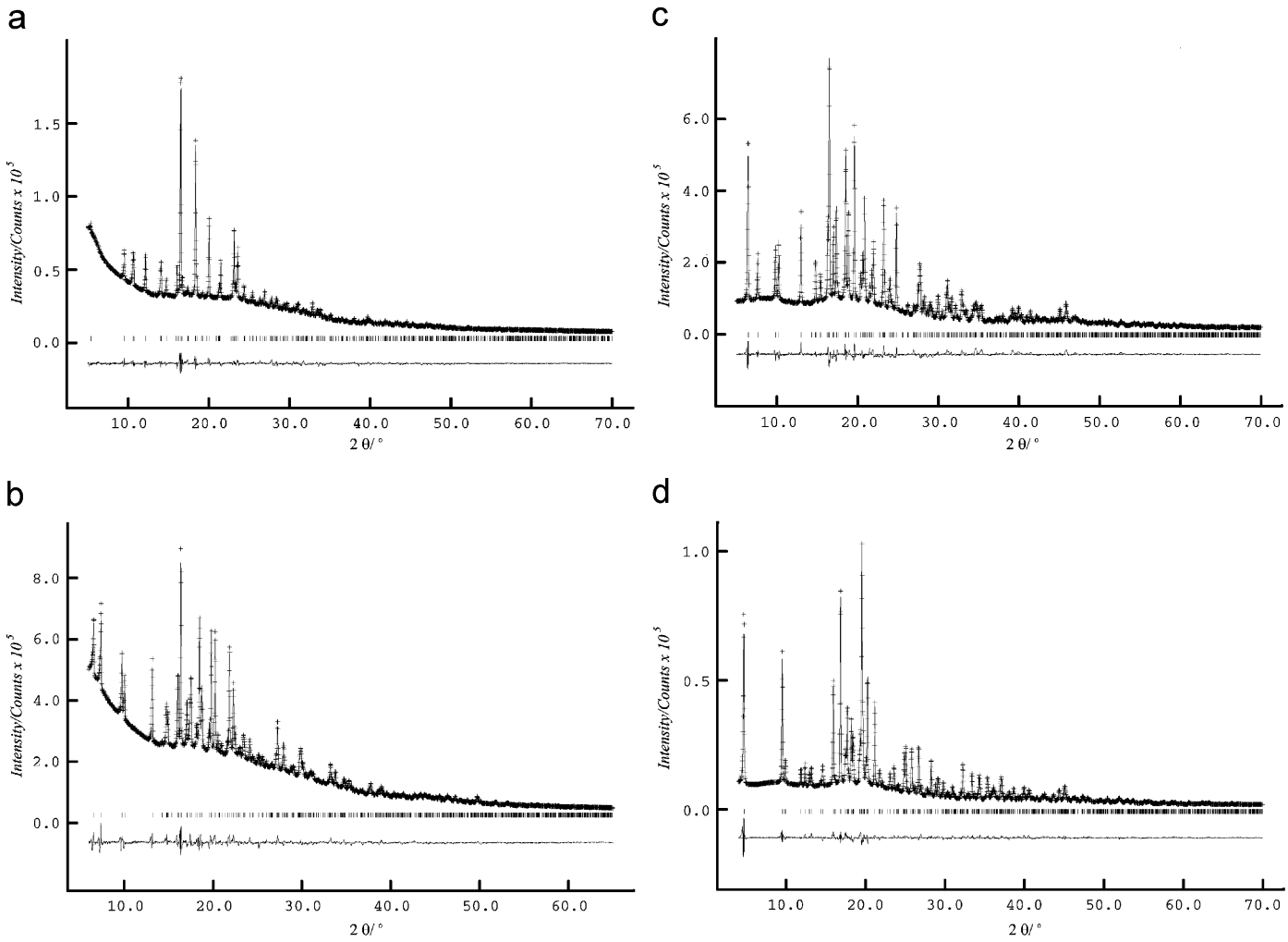

Fig. 3. Powder X-ray diffraction profiles for the final Rietveld refinements of (a) **1A**, (b) **1B**, (c) **1C**, and (d) **1D**. In each case, the experimental (+ marks), calculated (solid line) and difference (lower line) powder X-ray diffraction patterns are shown.

gave $R_{wp} = 0.0270$, $R_p = 0.0194$, $R_{F^2} = 0.288$ and $\chi^2 = 3.67$ [$C2/c$; $a = 26.8776(11)$ Å, $b = 6.36948(31)$ Å, $c = 23.9178(12)$ Å, $\beta = 91.7344(29)^\circ$].

The powder X-ray diffraction pattern of **1C** was indexed using the program ITO [13], giving the following unit cell ($M_{20} = 9.6$, $F_{20} = 26.3$) with monoclinic metric symmetry: $a = 27.05$ Å, $b = 6.31$ Å, $c = 22.86$ Å, $\beta = 92.3^\circ$ ($V = 3898$ Å^3). From systematic absences, the space group was assigned as $C2/c$. Le Bail fitting using this unit cell gave an acceptable fit to the experimental powder X-ray diffraction pattern ($R_{wp} = 0.0482$, $R_p = 0.0372$). Structure solution was carried out using a single-population GA implemented in the program EAGER, with two structural fragments in the asymmetric unit. The structural fragment representing **1** was defined by 12 structural variables (see above), and the structural fragment representing **C** was defined by eight structural variables, including two variable torsion angles (Fig. 2). Thus, the total number of structural variables in the GA calculation was 20. The best trial structure ($R_{wp} = 0.117$), obtained after 81 generations, was used as the initial structural model for Rietveld refinement. In the Rietveld refinement, standard restraints on bond lengths and bond angles were used, and both positional parameters and atomic displacement parameters were refined. Hydrogen atoms were placed in calculated positions towards the final stages of the refinement. The final refinement (Fig. 3c) gave $R_{wp} = 0.0484$, $R_p = 0.0358$, $R_{F^2} = 0.132$ and $\chi^2 = 4.09$ [$C2/c$; $a = 27.0843(10)$ Å, $b = 6.32418(24)$ Å, $c = 22.8922(8)$ Å, $\beta = 92.2766(22)^\circ$].

The powder X-ray diffraction pattern of **1D** was indexed using the program DICVOL [14], giving the following unit cell ($M_{20} = 41.4$, $F_{20} = 129.0$) with monoclinic metric symmetry: $a = 18.457$ Å, $b = 10.012$ Å, $c = 10.964$ Å, $\beta = 97.4^\circ$ ($V = 2009$ Å^3). From systematic absences, the space group was assigned as $P2_1/c$. Le Bail fitting using this unit cell gave a good fit to the experimental powder X-ray diffraction pattern ($R_{wp} = 0.0329$, $R_p = 0.0212$). Structure solution was carried out using a parallel GA implemented in the program EAGER, with two structural fragments in the asymmetric unit. The structural fragment representing **1** was defined by 12 structural variables (see above), and the structural fragment representing **D** was defined by nine

structural variables, including three variable torsion angles (Fig. 2). Thus, the total number of structural variables in the GA calculation was 21. The best trial structure ($R_{wp} = 0.123$), obtained after 75 generations, was used as the initial structural model for Rietveld refinement, which was carried out as described above for **1D**. The final refinement (Fig. 3d) gave $R_{wp} = 0.0425$, $R_p = 0.0299$, $R_{F^2} = 0.116$ and $\chi^2 = 3.79$ [$P2_1/c$; $a = 18.4999(5)$ Å, $b = 10.03765(19)$ Å, $c = 10.99568(21)$ Å, $\beta = 97.3784(13)^\circ$].

5. Results and discussion

Given the functional groups present in the molecules **1** and **A**–**D**, it is anticipated that hydrogen bonding should represent a significant feature of the crystal structures of the co-crystals **1A**–**1D**. Thus, in each structure, the cation [i.e. the protonated molecule $(HOCH_2)_n(CH_3)_{3-n}CNH_3^+$] has three N–H bonds, each of which is a potential hydrogen bond donor, and n O–H bonds, each of which is *both* a potential hydrogen bond donor *and* a potential hydrogen bond acceptor. The anion (i.e. deprotonated **1**), on the other hand, has three plausible hydrogen bond acceptors—the two oxygen atoms of the carboxylate group (each of which is capable of accepting more than one hydrogen bond) and the oxygen atom of the ether linkage. In practice, it is found that the oxygen atom of the ether linkage does not act as a hydrogen bond acceptor in any of the structures investigated.

Comparison of the unit cell dimensions of **1A**–**1D** reveals that the shortest unit cell axis is very similar (ca. 6.3–6.5 Å) in three of the co-crystals studied (**1A**, **1B** and **1C**), suggesting that these co-crystals may share a common crystal packing motif. As discussed below, this common short axis arises from the formation of chains of alternating gemfibrozil anions and *t*-butylammonium cations linked by N–H···O hydrogen bonds. Co-crystal **1D**, on the other hand, has a substantially different hydrogen bonding scheme.

In the crystal structure of **1A** (Fig. 4), the cation $(CH_3)_3CNH_3^+$ (i.e. protonated **A**) has the three N–H bonds of the $-NH_3^+$ group as hydrogen bond donors, and the anion (i.e. deprotonated **1**) has the two oxygen atoms of the

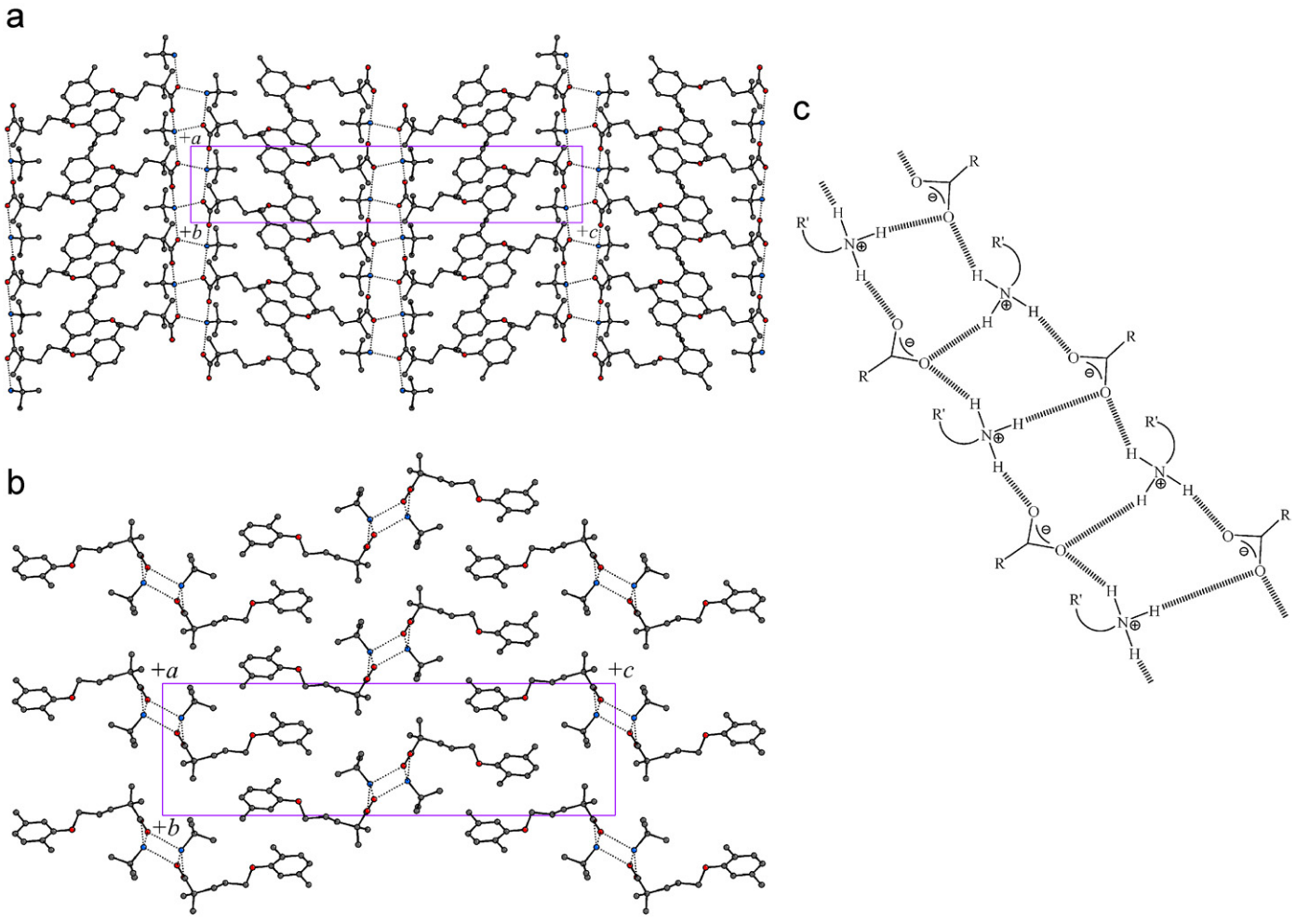

Fig. 4. (a) Crystal structure of **1A** viewed along the *b*-axis. Hydrogen bonds are indicated by dotted lines, and hydrogen atoms are omitted for clarity. Hydrogen bonded chains of alternating molecules of **1** and **A** run along the *a*-axis (vertical), and each pair of adjacent chains is cross-linked by further hydrogen bonding. (b) Crystal structure of **1A** viewed along the *a*-axis (the direction of propagation of the hydrogen-bonded chains). (c) Schematic diagram showing the hydrogen-bonding scheme in **1A**.

carboxylate group as hydrogen bond acceptors. The structure comprises chains of alternating molecules of **1** and **A** along the *a*-axis (periodic repeat distance 6.45 Å), with each pair of adjacent molecules in this chain linked by an N–H···O hydrogen bond. Each carboxylate oxygen atom of **1** is the acceptor in an N–H···O hydrogen bond within such a chain, and the $-NH_3^+$ group of **A** contributes two N–H bonds to the chain. The remaining N–H bond of the $-NH_3^+$ group forms an N–H···O(**1**) hydrogen bond to a carboxylate oxygen atom of a molecule of **1** in an adjacent chain, thus effectively providing a cross-link between adjacent chains. Each molecule of **1** receives one cross-linking N–H···O hydrogen bond from an adjacent chain in this manner. Pairs of adjacent chains are exclusively cross-linked to each other, and do not form cross-links to any other chain (as clearly seen from the view of the structure along the *b*-axis; Fig. 4a). As shown in Fig. 4c, the cross-linked pairs of hydrogen-bonded chains resemble a ladder-like arrangement, with the chains representing the frame of a ladder and the cross-links representing the rungs of the ladder. The two chains of the ladder and an adjacent pair of rungs give rise to a hydrogen-bonded ring, which is designated $R_4^3(10)$ in graph set notation [15]. Sets of cross-linked chains interact with each other through van der Waals interactions (Fig. 4b).

In the crystal structure of **1B** (Fig. 5), the OH group of the cation $(HOCH_2)(CH_3)_2CNH_3^+$ (i.e. protonated **B**) provides additional potential for hydrogen bonding (both as donor and acceptor) in comparison with the corresponding cation in **1A**. The structure contains chains of alternating molecules of **1** and **B** along the shortest unit cell axis (*b*-axis; periodic repeat distance 6.37 Å), with each pair of adjacent molecules in the chain linked by an N–H···O hydrogen bond (Fig. 5b). As in the structure of **1A**, pairs of chains are cross-linked to each other to form a ladder type structure, but the cross-linking is different from that in **1A**. Thus, instead of the single N–H···O(**1**) hydrogen bond that forms the rungs of the ladder in **1A**, the rungs of the ladder in **1B** involve a hydrogen bonding arrangement of the type N–H···O–H···O(**1**) in which the O–H group is from a molecule of **B**. For a given carboxylate group of **1**, only one oxygen atom is involved in a cross-linking interaction of this type. A given molecule of **B** acts as a hydrogen bond donor in N–H···O and O–H···O interactions that are formed to the *same* carboxylate group of **1** (but to different oxygen atoms of this carboxylate group), with the N–H···O(**1**) hydrogen bond forming part of the chain along the *b*-axis and the O–H···O(**1**) hydrogen bond forming part of the cross-linking rung of the ladder. A hydrogen bonded ring is formed by the two chains of the ladder and an adjacent pair of rungs, and is designated as $R_6^6(16)$ in graph set notation. As in the structure of **1A**, pairs of neighboring chains are exclusively cross-linked to each other (see Fig. 5a), and do not form cross-links to any other chain. Sets of cross-linked chains interact with each other through van der Waals interactions.

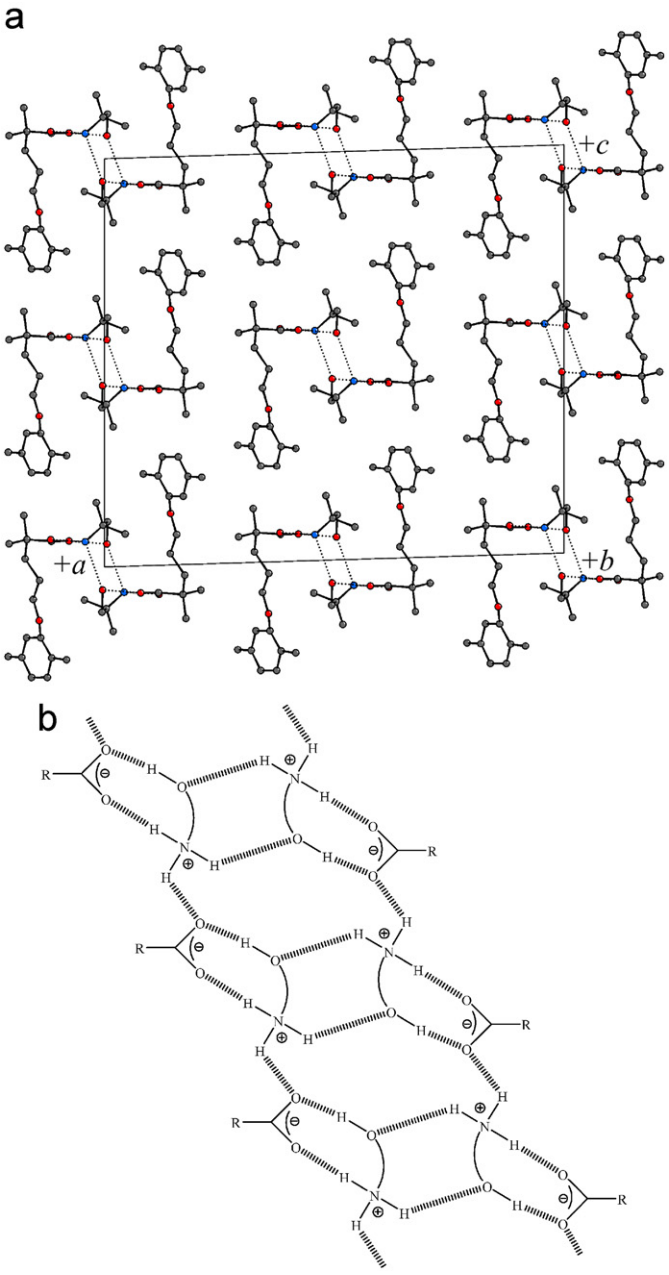

Fig. 5. (a) Crystal structure of **1B** viewed along the *b*-axis (the direction of propagation of the hydrogen-bonded chains). Hydrogen bonds are indicated by dotted lines, and hydrogen atoms are omitted for clarity. (b) Schematic diagram showing the hydrogen-bonding scheme in **1B**.

In the crystal structure of **1C** (Fig. 6), the cation $(HOCH_2)_2(CH_3)CNH_3^+$ now has two OH groups, creating further opportunities for hydrogen bonding in comparison with **1A** and **1B**. Indeed, each of the five potential hydrogen bond donors in **C** (i.e. three N–H bonds and two O–H bonds) is involved in an N–H···O or O–H···O hydrogen bond. As in **1A** and **1B**, hydrogen bonded chains are formed along the shortest unit cell axis (*b*-axis; periodic repeat distance 6.32 Å), involving alternating molecules of **1** and **C**. Within the chain, each pair of adjacent molecules is linked by an N–H···O hydrogen bond. Each carboxylate

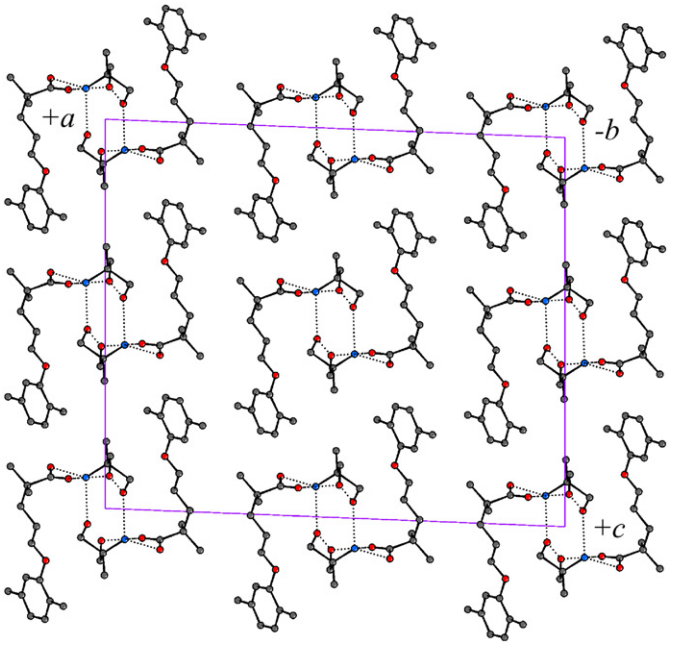

Fig. 6. Crystal structure of **1C** viewed along the *b*-axis (the direction of propagation of the hydrogen bonded chains). Hydrogen bonds are indicated by dotted lines, and hydrogen atoms are omitted for clarity.

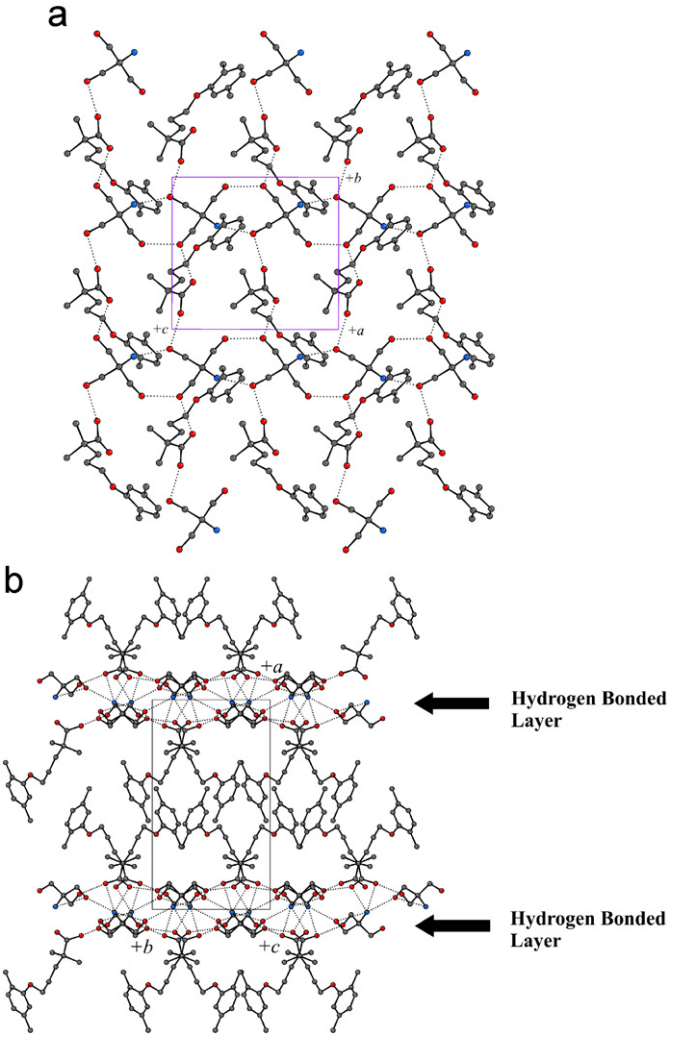

Fig. 7. (a) A single hydrogen bonded layer within the crystal structure of **1D** viewed along the *a*-axis (perpendicular to the plane of the layer). (b) Crystal structure of **1D** viewed along the *c*-axis, showing the layered nature of the structure. Hydrogen bonds are indicated by dotted lines, and hydrogen atoms are omitted for clarity. Hydrogen bonded layers containing the molecules of **D** and the carboxylate groups of molecules of **1** are indicated. The remainder of each molecule of **1** projects into the region of space between adjacent layers.

oxygen atom of **1** is involved in one N–H···O hydrogen bond within the chain, and two N–H bonds of each $-NH_3^+$ group are involved in the N–H···O hydrogen bonds within the chain. A ladder-type structure is again formed by cross-linking of neighboring chains, but each cross-link now involves a hydrogen bonding arrangement of the type N–H···O–H···O–H···O(**1**). For a given carboxylate group of **1**, only one oxygen atom is involved in a cross-linking interaction of this type, and for each $-NH_3^+$ group, one N–H bond is involved in such cross links. For a given cross-link, the two O–H groups are from different molecules of **C**. The two chains of the ladder and an adjacent pair of rungs give rise to a hydrogen bonded ring, designated $R_8^8(20)$ in graph set notation. The rungs are not straight, but form a twisted path. As in the crystal structures of **1A** and **1B**, pairs of neighboring chains are exclusively cross-linked to each other, and not to any other chain (see Fig. 6). Adjacent sets of cross-linked chains are in van der Waals contact with each other.

In the crystal structure of **1D** (Fig. 7), the cation $(HOCH_2)_3CNH_3^+$ has three OH groups, in addition to the three N–H hydrogen bond donors, representing a total of six potential hydrogen bond donors. It might be expected that the crystal structure should have three N–H···O(**1**) hydrogen bonds, in accordance with the general rule that the strongest hydrogen bond donor interacts with the strongest hydrogen bond acceptor [16], as observed in the crystal structures of **1A**, **1B** and **1C**. However, the crystal structure has only one N–H···O(**1**) hydrogen bond. Thus, one carboxylate oxygen atom of **1** is not involved in an N–H···O hydrogen bond, but is instead involved as the acceptor in an O–H···O(**1**) hydrogen bond, with a hydroxyl group of **D** as the donor. Each of the other two N–H donors of **D** forms an N–H···O(**D**) hydrogen bond (with a hydroxyl group of **D** as the acceptor), and there are also two O–H···O(**D**) hydrogen bonds. In total, there are six independent types of hydrogen bond in the structure, with one carboxylate oxygen atom of **1** acting as an acceptor for two hydrogen bonds. The numerous hydrogen bonding interactions give rise to extensively hydrogen-bonded sheets parallel to the *bc*-plane (see Fig. 7a), involving the cations of **D** and the carboxylate groups of **1**. The other (non-carboxylate) parts of the gemfibrozil molecules extend outwards from both faces of the sheet, and the region between adjacent sheets is dominated by van der Waals interactions between the gemfibrozil molecules. The arrangement of molecules in the

crystal structure of **1D** clearly differs substantially from those in **1A**, **1B** and **1C**, which share several structural similarities as discussed above. Thus, instead of forming infinite hydrogen bonded chains, with cross-linking between pairs of adjacent chains, the structure of **1D** comprises a two-dimensional sheet-like network of hydrogen bonding interactions.

6. Concluding remarks

The complexities of the crystal structures unravelled in the present work from powder X-ray diffraction data recorded on a standard laboratory powder X-ray diffractometer are indicative of the growing power and scope of current methodology for carrying out complete structure determination of organic molecular materials directly from powder X-ray diffraction data. Analysis of the intermolecular interactions that govern the structural properties of organic molecular crystals, coupled with careful studies of mechanical and physical properties of these materials, is a pre-requisite for establishing correlations between structural characteristics and physical properties. We emphasize that obtaining a fundamental understanding of such structure-property relationships can be crucially important in the development and optimization of materials for industrial applications, including those of relevance to pharmaceuticals industries.

Acknowledgments

We thank Bristol-Myers Squibb (studentship to SED) and E.P.S.R.C. (general support to KDMH and post-doctoral fellowship to EYC) for financial support.

References

[1] (a) P.A. Todd, A. Ward, Drugs 36 (1988) 314;
(b) S.R. Wirebaugh, M.L. Shapiro, T.H. McIntyre, E.J. Whitney, Pharmacotherapy 12 (1992) 445.
[2] (a) K.D.M. Harris, M. Tremayne, Chem. Mater. 8 (1996) 554;
(b) K.D.M. Harris, M. Tremayne, B.M. Kariuki, Angew. Chemie Int. Ed. 40 (2001) 1626;
(c) V.V. Chernyshev, Russian Chem. Bull. 50 (2001) 2273;
(d) W.I.F. David, K. Shankland, L.B. McCusker, C. Baerlocher (Eds.), Structure Determination from Powder Diffraction Data, OUP/IUCr, 2002.;
(e) K.D.M. Harris, E.Y. Cheung, Chem. Soc. Rev. 33 (2004) 526;
(f) M. Tremayne, Phil. Trans. Roy. Soc. 362 (2004) 2691;
(g) A. Altomare, R. Caliandro, M. Camalli, C. Cuocci, C. Giacovazzo, A.G.G. Moliterni, R. Rizzi, R. Spagna, J. Gonzalez-Platas, Z. Kristallogr. 216 (2004) 833;
(h) V. Favre-Nicolin, R. Černý, Z. Kristallogr. 216 (2004) 847;
(i) K. Shankland, A.J. Markvardsen, W.I.F. David, Z. Kristallogr. 216 (2004) 857;
(j) R. Černý, Croat. Chem. Acta 79 (2006) 319.
[3] K.D.M. Harris, M. Tremayne, P. Lightfoot, P.G. Bruce, J. Am. Chem. Soc. 116 (1994) 3543.
[4] (a) B.M. Kariuki, H. Serrano-González, R.L. Johnston, K.D.M. Harris, Chem. Phys. Lett. 280 (1997) 189;
(b) K.D.M. Harris, R.L. Johnston, B.M. Kariuki, Acta Crystallogr. A 54 (1998) 632;
(c) S. Habershon, K.D.M. Harris, R.L. Johnston, J. Comp. Chem. 24 (2003) 1766;
(d) K.D.M. Harris, S. Habershon, E.Y. Cheung, R.L. Johnston, Z. Kristallogr. 216 (2004) 838.
[5] (a) H.M. Rietveld, J. Appl. Crystallogr. 2 (1969) 65;
(b) R.A. Young (Ed.), The Rietveld Method, International Union of Crystallography, Oxford, 1993;
(c) L.B. McCusker, R.B. Von Dreele, D.E. Cox, D. Louër, P. Scardi, J. Appl. Crystallogr. 32 (1999) 36.
[6] (a) S.M. Berge, L.D. Bighley, D.C. Monkhouse, J. Pharm. Sci. 66 (1977) 1;
(b) D.A. Adsmond, D.J.W. Grant, J. Pharm. Sci. 90 (2001) 2058;
(c) D. Giron, J. Pharm. Sci. 73 (2003) 441;
(d) S.L. Morisette, O. Almarsson, M.L. Peterson, J.F. Remenar, M.J. Read, A.V. Lemmo, S. Ellis, M.J. Cima, C.R. Gardner, Adv. Drug. Deliv. Rev. 56 (2004) 275;
(e) O. Almarsson, M.J. Zaworotko, Chem. Commun. (2004) 1889;
(f) A.V. Trask, W.D.S. Motherwell, W. Jones, Cryst. Growth Des. 5 (2005) 1013;
(g) P. Vishweshwar, J.A. McMahon, J.A. Bis, M.J. Zaworotko, J. Pharm. Sci. 95 (2006) 499.
[7] G.S. Pawley, J. Appl. Crystallogr. 14 (1981) 357.
[8] A. Le Bail, H. Duroy, J.L. Fourquet, Mater. Res. Bull. 23 (1988) 452.
[9] S. Habershon, G.W. Turner, Z. Zhou, B.M. Kariuki, E.Y. Cheung, A.J. Hanson, E. Tedesco, D. Albesa-Jové, M.-H. Chao, O.J. Lanning, R.L. Johnston, K.D.M. Harris, EAGER—A Computer Program for Direct-Space Structure Solution from Powder X-ray Diffraction Data, Cardiff University and University of Birmingham, 2006.
[10] A.C. Larson, R.B. Von Dreele, GSAS, Los Alamos Laboratory Report No. LA-UR-86-748, 1987.
[11] K.M. O'Connor, O.I. Corrigan, Int. J. Pharm. 222 (2001) 281.
[12] F. Kohlbeck, E.M. Hörl, J. Appl. Crystallogr. 9 (1976) 28.
[13] J.W. Visser, J. Appl. Crystallogr. 2 (1969) 89.
[14] (a) A. Boultif, D. Louër, J. Appl. Crystallogr. 24 (1991) 987;
(b) A. Boultif, D. Louër, J. Appl. Crystallogr. 37 (2004) 724.
[15] (a) M.C. Etter, Acc. Chem. Res. 23 (1990) 120;
(b) M.C. Etter, J.C. MacDonald, J. Bernstein, Acta Crystallogr. B 46 (1990) 256;
(c) J. Bernstein, R.E. Davis, L. Shimoni, N.L. Chang, Angew. Chemie Int. Ed. 34 (1995) 1555.
[16] M.C. Etter, J. Phys. Chem. 95 (1991) 4601.